Photovoltaic-Battery Systems Design to Improve the Self-Sufficiency of Telecommunication Towers

Photovoltaic-Battery Systems Design to Improve the Self-Sufficiency of Telecommunication Towers

Alessandro Ciocia, Angela Amato, Paolo Di Leo, Gabriele Malgaroli, Gianluca Sbriglia, Filippo Spertino
Dipartimento Energia "Galileo Ferraris", Politecnico di Torino
Torino, Italy
{alessandro.ciocia, gabriele.malgaroli, angela.amato, paolo.dileo, filippo.spertino}@polito.it, gianluca.sbriglia@studenti.polito.it

***Abstract*—The goal of the present work is to maximize the self-sufficiency of power needs for telecommunication stations by installing PhotoVoltaic (PV) systems. The available land for PV installation in areas with telecommunication towers is, generally, poor, and a proper sizing procedure is required. In this work, it is supposed to dismiss the old telecommunication tower of three sites and install properly designed towers. Three types of towers with different active PV surfaces are analyzed for each site using 3D models. Then, energy balances and financial parameters are calculated and compared, demonstrating the feasibility of the investment. For one of the towers under analysis, the integration of a storage system is investigated by estimating its energy and economic benefits.**

Keywords—Photovoltaic plant, battery storage system, telecommunication systems, designed towers, self-sufficiency, self-consumption.

I. INTRODUCTION

In future, most of the electricity users will have local renewable generators, in order to reduce the pollution. Among the renewables technologies, PhotoVoltaic (PV) generation is the most promising. First, PV systems are easy scalable; thus, they can be designed to meet the demand of small domestic users (few kW), up to the big factories (multi-MW). Another key point is the possibility to be installed in areas without available land: PV modules can be installed on the rooftops of the buildings [1] or integrated in walls, windows, balconies, etc. New plants are often equipped with multiple Maximum Power Point Tracking systems (MPPT) to increase the performance in case of shadows [2] from objects in the neighbourhood or in case of high electrical mismatch [3]. Finally, other two factors that increased the use of this technology in the last two decades are the decrease of PV costs, and the improvement in its efficiency. In the following papers, the most interesting applications for PV-storage systems in the telecommunications sector are presented. The techno-economic feasibility of the "grid, PV generators and storage" configuration as a possible power supply for telecom tower loads is analyzed in [4]. Moreover, in [5], a control algorithm for a PV-storage system is developed with the aim of reducing the dependency of telecommunications sector on diesel generators. Finally, in [6], a multi-objective optimization algorithm is proposed to size the components of a standalone PV-storage system for a mobile network base station. In the present work, PV generators and storage systems are sized to meet the electrical demand of telecommunication stations. The goal is to reduce their use of electricity from fossil fuels with cost effectiveness: thus, both technical and economical constraints are considered. In particular, the available space for the installation of the PV system is poor with a relatively high consumption. Thus, a key point is the installation of the PV generator on the telecommunication towers. The replacement of the old towers with new commercial ones is considered, and 3D models of the new towers are used to avoid shadows on the PV models.

II. MODELLING OF PV GENERATORS AND BATTERIES

An appropriate simulation procedure to design the electric supply of the telecommunication towers has been set up with respect to PV generators and batteries, modelled as functions of time with hourly update.

A. Photovoltaic production model

The PV power production is simulated according to the following model described in [7]:

$$P_{AC} = P_{PV} \cdot \frac{G-G_0}{G_{STC}} \cdot \eta_{th} \cdot \eta_{DC/AC} \cdot \eta_{mix} \quad (1)$$

The AC power production P_{AC} from a PV generator is proportional to the solar irradiance G and depends on ambient temperature T_a. Losses due to low irradiance are taken into account by using the quantity G_0, which is subtracted to the irradiance G. The quantity (G-G_0) irradiance is normalized to the reference irradiance in Standard Test Condition (STC) G_{STC} [8]. The efficiency of DC/AC converter and thermal losses η_{th} are variable in time, while the other sources of losses are assumed constant and grouped in the factor η_{mix}. In particular, this quantity takes in consideration the Joule losses in wires, the losses due to glass reflection in the PV modules, mismatch in the characteristic curve of the PV modules, and the accuracy of the MPPT systems. Regarding the thermal losses, the performance reduction is proportional to a thermal coefficient γ_{th} and to the difference between the module temperature T_m and the STC temperature T_{STC}=25 °C:

$$\eta_{th} = 1 + \gamma_{th} \cdot (T_m - T_{STC}) \quad (2)$$

In literature, different correlations permit to estimate the module temperature T_m starting from the knowledge of the air temperature. For each PV module, the manufacturer must provide the Normal Operating Cell Temperature (*NOCT*), which is the temperature reached by PV modules with $T_{a,NOCT}$=20 °C, G_{NOCT}=800 W/m^2, and wind speed of 1 m/s. The module temperature can be assessed by this relationship:

$$T_m = T_a + G/G_{\mathrm{NOCT}} \cdot (NOCT - T_{\mathrm{a,NOCT}}) \quad (3)$$

Finally, the DC/AC converter efficiency is the ratio between its output AC power and its input DC power:

$$\eta_{inv} = \frac{P_{AC}}{P_{DC}} = \frac{P_{DC} - P_{loss}}{P_{DC}} \quad (4)$$

$$P_{loss} = P_0 + C_L \cdot P_{DC} + C_Q \cdot P_{DC}^2 \quad (5)$$

where P_{loss} is the lost power calculated as a parabolic function: the standby losses P_0 are the constant contribution, the linear contribution is the conduction of the diodes C_L, and the quadratic contribution is the resistive term C_Q.

B. Minimum distance between modules

In the present work, the installation of PV modules on the vertical surfaces of telecommunication towers in Italy is simulated. Modules can be installed vertically, or with a lower tilt using proper metallic structures, similarly to sunblinds. This inclination is selected to increase the yearly energy production with respect to vertical installations. To avoid any shading on the modules, the angle corresponding to the maximum sun height is calculated during the summer solstice. Then, the minimum distance at which the PV modules can be placed on the towers is determined as follows:

$$d_{min} = m \cdot \cos\beta \cdot \tan\alpha \quad (6)$$

where d_{min} is the minimum distance between PV modules; m and h are the length and the height of each module, respectively. The parameter β is the tilt angle of the module, and α is the elevation angle of the sun. As a result, the minimum distance between PV modules is the sum between h and d_{min}. For the sake of clarity, these geometrical quantities are represented in Fig.1.

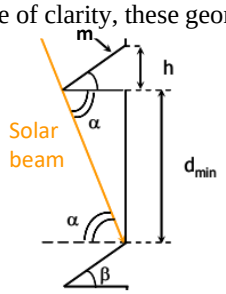

Fig. 1. Geometrical quantities of vertical modules receiving solar beams.

C. Electrochemical storage modelling

The energy model of batteries is based on their State of Charge (*SOC*) [9]. For each time instant *t*, *SOC*(*t*) must be in the range SOC_{min}–SOC_{max}. In fact, an overcharge $SOC(t) > SOC_{max}$ or a deep discharge $SOC(t) < SOC_{min}$ may reduce the performance of batteries, as well as their useful life, leading to their failure. The quantity *SOC*(*t*) depends on its value at the previous time instant, on the charging efficiency $\eta_{bat,c}$, and on the nominal energy capacity C_{bat}. The energy injected or absorbed by the battery is the product of the average power during the selected time step Δt and the time step. The formula, in case of charge is the following:

$$SOC(t) = SOC(t-1) + \left(\frac{|P_{bat}| \cdot \Delta t}{C_{bat} \cdot \eta_{bat,c}}\right) \quad (7)$$

In discharge, instead, the equation is the following:

$$SOC(t) = SOC(t-1) - \left(\frac{|P_{bat}| \cdot \Delta t}{C_{bat}}\right) \quad (8)$$

D. Self-sufficiency and self-consumption

Two indicators quantifying how much energy is produced and consumed locally are the Self-Sufficiency (*SS*) and the Self-Consumption (*SC*) [10], which are defined in the following way:

- Self-sufficiency is the ratio between the energy locally produced and immediately used E_{lpc} (or locally stored and then used) by the consumer, and the load (E_{load}).

$$SS = E_{lpc}/E_{load} \quad (9)$$

- Self-consumption is the ratio of the energy locally produced and immediately used E_{lpc} (or locally stored and then used) by the consumer, to the generation (E_{gen}).

$$SC = E_{lpc}/E_{gen} \quad (10)$$

For the sake of clarity, the energy E_{lpc} is represented in Fig. 2: at each time step, this quantity is the minimum between the production and the load. The remaining production is the surplus energy that can be injected into the grid; the remaining load is the deficit, i.e. the part of the load to be fulfilled by absorbing energy from the grid.

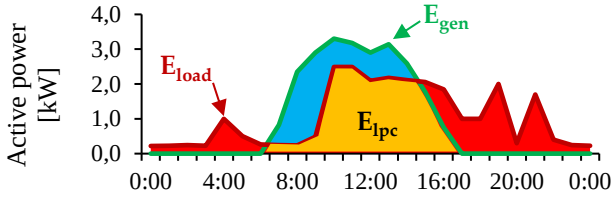

Fig. 2. Example of daily profile with hourly time step.

The *SC* is, generally, high in case of undersized plants: in such condition, the generation peak is, generally, lower than the load, and most of local production is immediately consumed. However, an undersized plant has low energy production, and cannot satisfy the whole load using renewable energy, with a consequent low *SS* (and, thus, with high absorption from the grid). On the contrary, an oversized plant generally produces more power than the requested amount to fulfil the load: in this case, *SS* is high, as well as the energy injection into the grid, with a consequent low *SC*. As a conclusion, the PV plant is properly sized, i.e., its production well matches the load, when both *SC* and *SS* are high.

E. Improvement of self-sufficiency

In order to increase the self-sufficiency, PV energy used to satisfy local loads has to be improved, lowering the energy injection into the grid. The compensation is performed in different ways according to the country. A first distinction is based on compensation time. The mechanisms created to compensate the mismatch between production and consumption of energy in real time (or in time intervals up to 15 min) are named "self-consumption schemes". If the compensation occurs in a larger time frame, they are "net-metering schemes". Another methodology is the compensation on cash-flow basis (rather than on energy basis): in this situation, the mechanism is called "net-billing scheme". In some cases, these programs are hybrids of the abovementioned main schemes. In Italy, a net billing system (based on compensation during the whole year) is currently working for PV systems up to 500 kW. No feed-in tariffs for new plants are included, but a tax discount of 50 % of the investment (5 % per year in 10 years) is available for small-medium size PV systems [11].

F. Financial feasibility

The Net Present Value (*NPV*) is an economic parameter taking into account, at each year *t*, the revenues R_t, the negative cash flows (e.g., costs of maintenance) C_t, and the investment cost *IC*. Cash flows are discounted with $(1+i)^t$. The discount rate *i* is generally low (2%–4%), because the investment in PV systems has low risk and long duration. The number of years *n* is the investment lifetime, as shown in (11):

$$NPV = -IC + \sum_{t=1}^{n} \left(\frac{R_t - C_t}{(1+i)^t} \right) \qquad (11)$$

The Internal Rate of Return (*IRR*) is the discount rate that makes the *NPV* equal to zero; i.e., the interest rate that provides the balance between costs and revenues at the end of the useful life for the plant under analysis. In particular, the *NPV* equation is set equal to zero in order to evaluate *i*:

$$\sum_{t=1}^{n} \left(\frac{R_t - C_t}{(1+i)^t} \right) - IC = 0 \qquad (12)$$

The main difference in the two above-described terms is that the *NPV* provides the economic return of the investment, but it is not the best solution to compare investments. On the contrary, the *IRR* is useful to compare different kinds of investments. For example, in case of the comparison regarding the installation of two plants with different rated powers, the *NPV* might be higher for the biggest plant. Nevertheless, the economic effectiveness of the investment might be higher for the plant with the lower size [12]. This situation might be the comparison between the investments in an oversized plant, and in a properly sized plant.

III. Sizing Procedure for PV-Battery Systems

The procedure to size a PV-battery system is summarized in Fig. 3. The goal is the definition of the optimal size to reach the highest self-sufficiency or the maximum economic return. Each step is described in the following sub-paragraphs.

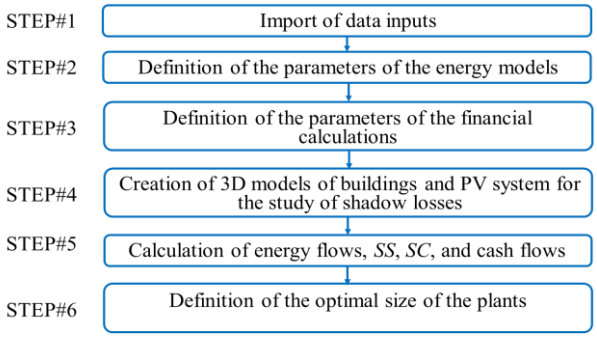

Fig. 3. Flow chart of the procedure for the sizing of the PV-battery system.

A. Step 1: Import of data inputs

The first step is the definition of import data. Therefore, information about the installation location, meteorological data (temperature, irradiance and wind speed, if available, can be downloaded from public and private databases) are obtained. As an example, a large part of the globe is available in the PVGIS database [13]. This database makes values on an hourly basis available, for a set of 12 years (depending on the location). These profiles are the result of the processing of satellite data and measurements detected by ground weather stations. Another key input is to obtain the electricity consumption data of the users or of the equipment under consideration. In the present case, the consumption data of the telecommunications towers were measured. If measurements are not available, proper databases can be used to obtain typical consumption profiles [14].

B. Step 2: Definition of the parameters of energy models

In the second step of the procedure, the parameters of the energy models are defined. In the present work, the parameters are selected as follows. Regarding the PV production calculation, the thermal losses with respect to the STC conditions are $\gamma_{th} \approx$ -0.5 %/°C, while the *NOCT*=45 °C [15]. Losses due to reflection can be considered equal to about 3 %. Mismatch losses due to non-uniformity in *I-V* characteristic curves of PV modules lead to losses that can be assumed constant and equal to ≈3 %. Losses due to low irradiance are taken into account by setting the limit G_{lim}=0.018 kW/m^2, which represents the minimum level of irradiance needed to turn on the inverter. Joule losses in cables and losses due to limited MPPT accuracy lead to 1 % of efficiency reduction. Regarding the DC/AC converter, the losses P_0, C_L and C_Q are equal to 0.7 % of the nominal power each, when the converter works at full load [16]. Concerning the storage model, a typical maximum number of discharge-charge cycles values for commercial batteries is 10000 with DOD=80 %, but the batteries life, generally, may be much longer. Even if the maximum number of cycles is not achieved, after ≈10 years the batteries are anyway replaced. This operation is performed in order to ensure the correct working of the system. Finally, the useful life of PV modules is supposed to be 25 years and the annual losses due to the aging of the plants is -0.5 %/year [17][18]. The average life of AC/DC converters is about 10 years.

C. Step 3: Definition of the financial parameters

The third step concerns the definition of the financial parameters. PV systems are modular; therefore, their installation cost should be quite constant. Nevertheless, there are fixed costs, which impact mainly in small PV plants; the unitary cost of standard crystalline PV modules and inverters decreases in case of big plants. In case of small plants (rated power of about few kW), the installation cost is about 2 k€/kW, while this term decreases down to 1.1−1.2 k€/kW in case of few MW plants, and it can be lower than 0.65 k€/kW for multi-MW systems [19]. Regarding the storage, the installation cost of Li-ion batteries is supposed in the range 300−400 €/kWh [20]. A minimum *IRR* of 6 % is considered as limit for the effectiveness of the investments in renewable sources [21]. In Italy, the price of electricity for small/medium commercial users is ≈16.5 c€/kWh, while the value of self-sufficiency is ≈11 c€/kWh. The selling price of electricity to the grid is 4 c€/kWh [22].

D. Step 4: 3D model of the plants for shadow analysis

Shadowing is one of the most important sources of losses in PV system. Firstly, the production is reduced by a quota that is proportional to the ratio between the shadowed area and the total irradiate surface of PV modules. This quota depends on the presence of bypass diodes, and on the series-parallel connection of the modules. Secondly, continuous shadings during the life of the plant lead to a thermal stress for the diodes, with an increased failure probability [23]. Finally, the MPPT operation is affected by this phenomenon because the identification of the maximum power point may fail by finding local power peaks. In fact, multiple articles in literature discuss mathematical methods to increase the efficiency in shading conditions [24][25]. The presence of multiple MPPTs, up to one MPPT for each module, is a solution even more used to reduce the losses due to shadows [26]. In the present work, the installation of PV modules is simulated on a specific application, i.e. communication towers: hence, a 3D model of towers and PV modules is created in PVsyst. This model permits to simulate the shadows and assess the energy losses. For the sake of simplicity, the production of the shadowed modules is null, thanks to the operation of bypass diodes. No reduction on the production of the other modules and on the MPPT efficiency is considered.

E. Step 5: Calculation of energy and cash flows

The fifth step of the procedure is the calculation of the energy and cash flows. Regarding the energy flows, the PV production is calculated, and the effect of shadows is taken into account. For each time step, the battery operation E_{bat} is calculated to balance generation E_{gen} and load E_{load} according to the technical constraints, e.g., the limits for the *SOC*. The storage has the priority over the grid; thus, only the remaining deficit/surplus E_{grid} is exchanged with the grid [27].

In the following formula, the active sign convention is used:

$$E_{\mathrm{load}} = E_{\mathrm{gen}} + E_{\mathrm{bat}} + E_{\mathrm{grid}} \qquad (13)$$

After the energy flows calculation, the self-sufficiency and self-consumption parameters are calculated, according to Section II. B. Finally, *NPV* and *IRR* are estimated.

F. Step 6: Optimal plants sizes definition

The last step of the procedure is the calculation of the optimal size for the PV generator and the storage. The calculation starts from a PV size suitable to produce an energy quantity equal to the annual load, while the initial storage capacity is sized to supply the load for an entire day without PV production. An iterative procedure changes the sizes of the plants and calculates, at each step, the energy and cash flows. Results are stored at each iteration, and the best result is selected. In literature, optimization methods are used to solve the sizing problem [28].

IV. Feasibility Study of PV-Storage Systems for Telecommunication Towers

The case study presented in this work is related to three existing telecommunication stations in Northern Italy. A typical station has a fenced area of 50−100 m^2 and includes a tower with antennas, and electronic equipment inside containers. Power is supplied by the LV distribution grid. The three telecommunication stations under analysis have the characteristics described in Table I. For the sake of clarity, an example of tower is shown in Fig. 4. An example of daily load profiles related to the first site is shown in Fig. 5. The consumption is quite constant during day/night with a base load of ≈5 kW. The peak occurs during daytime hours due to the conditioning of the containers. Fig. 5 shows that the shape of the load profiles is similar among seasons, with an increase (up to ≈9 kW) due to conditioning of the containers with electronic equipment. Site#1 is the most favorable case for production, because it is located in the plain, and the fenced area is south oriented.

TABLE I. Characteristics of Telecommunication Towers

Latitude	44°53'N (#1)	44°45'N (#2)	46°07'N (#3)
Tower height (m)	35	30	25
Site area (m^2)	59	132	103
Tower type	Truss	Pole	Truss
Load (kWh/year)	51.510	59.164	43.991
Tower azimuth (°)	0	+45	+40

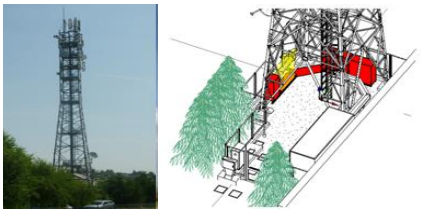

Fig. 4. Photo of the telecom tower in Site#1 and related 3D image.

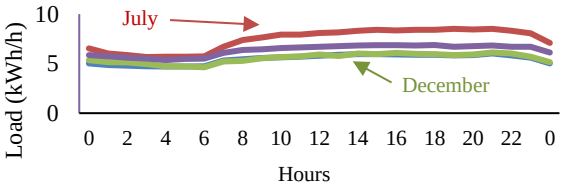

Fig. 5. Examples of daily profiles with hourly time step in Site#1.

Thus, it is possible to install a tower with an azimuth angle of 0°. On the contrary, Site#2 is surrounded by mountains and has a SO azimuth (≈40°) leading to a lower PV production. Moreover, this site has the highest electrical load. Site#3 is in plain area but has a SO azimuth equal to +45°; this site has the lowest load. In each site under analysis, the installation of new towers with different shapes is simulated. The goal is to identify the configuration with the highest self-sufficiency and economic return. The three towers are commercial, and have the following characteristics:

- (TW1) - triangular section, and 40 m height;
- (TW2) - hexadecagonal section, and 24 or 30 m height;
- (TW3) - hexagonal section, and 24 or 30 m height.

Regarding PV modules, in case of TW1 and TW3 the installation of commercial c-Si modules with high efficiency (≈22 %) is supposed. The modules have a standard size of 1 m x 1.7 m and a metallic frame for an adequate installation on the tower. On TW2, it is supposed to install customized modules (details are in the next subsections).

A. *Tower layout #1 (TW1)*

The first tower under analysis is made by wood, and it has a triangular section. As shown in Fig. 6, the tower can be installed with two orientations:

α - facing south with one of the three sides;
β - with two sides exposed to southeast and southwest with azimuth angles of +60° and -60°.

For each configuration, simulations are performed with two PV installations: in the first case, PV modules are applied on the faces of tower, while in the other they are installed on a canopy created on the container roof. In configuration α, PV modules on the tower are south oriented, but the available space is limited (the maximum number of modules is 32).

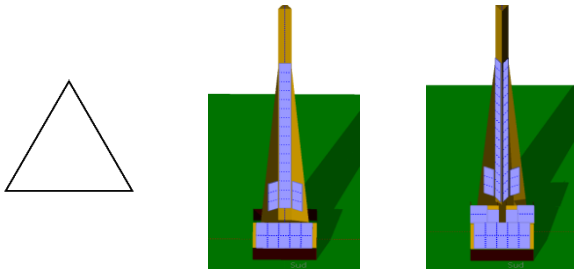

Fig. 6. Cross section of tower TW1 (left) and its possible orientations: with a face facing south (center) or with two faces facing southeast and southwest (right).

In the three sites, the *SS* is in the range 18–22 %. The *IRR* of the investments are in the range 3–5 %. The best energy results are obtained in the configuration β, in which 54 modules are installed, with worse azimuth angles. The *SS* is in the range 29–34 %, and the *IRR* is 3–5 %. Tables II and III show the main results of the two configurations for TW1. The results show that the *IRR* is lower than 6 %, due to the low PV production. If the modules are installed only on the canopy, the *IRR* of the investments is in the range 6–8 %, but the self-sufficiency is much lower (8−15 %).

TABLE II. RESULTS OF CONFIG. α IN THE THREE SITES (TW1)

	Site#1	Site#2	Site#3
PV power (kW)	11.8	11.8	11.8
Production (MWh/year)	12.2	11.0	10.6
Self-sufficiency (%)	22	18	22
IRR (%)	5.2	4.1	3.4
NPV (k€)	5.8	2.7	0.9

TABLE III. RESULTS OF CONFIG. β IN THE THREE SITES (TW1)

	Site#1	Site#2	Site#3
PV power (kW)	20	20	20
Production (MWh/year)	19.0	18.3	16.6
Self-sufficiency (%)	32	29	31
IRR (%)	5.2	4.9	3.4
NPV (k€)	8.8	7.7	1.4

B. Tower layout #2 (TW2)

The layout of the second tower is shown in Fig. 7. Two towers with a hexadecagonal section are considered: they have a height of 24 and 30 m, respectively. Standard modules cannot be installed on this kind of towers, because the faces width is <1 m, while standard modules are 1 x 1.7 m. Thus, the installation of custom modules with sizes 1.1 x 0.3 m is supposed. On the 24 m high tower, 46 modules can be installed, while on the 30 m high one, 68 modules can be applied. The faces are those oriented from south-east to south-west. Nevertheless, the investment and installation cost of custom modules is higher than standard modules (investment of ≈6 k€/kW). Standard modules can be installed on the canopy (Fig. 7). Due to the high price of custom modules, the *NPV* is negative for each possible configuration. Acceptable results are obtained only for traditional modules installed on the canopy in front of the tower (for a total of 24 modules). The results from the simulations are shown in Table IV.

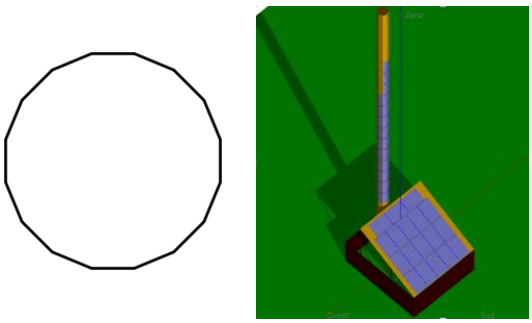

Fig. 7. Cross section of tower TW2 (left) and its 3D model with a canopy over the containers (right).

In these first two layouts (TW1 and TW2), the operation of the battery is not simulated. In fact, the installable plants are, generally, undersized with respect to the local loads due to the low available space. In a few cases, the sizes of the plants are more adequate, but the financial limit (*IRR*≥6 %) does not permit the installation of batteries.

TABLE IV. RESULTS FOR TW2 IN THE THREE SITES

	Site#1	Site#2	Site#3
PV power (kW)	8.9	8.9	8.9
Production (MWh/year)	12.8	11.3	11.1
Self-sufficiency (%)	24	19	24
IRR (%)	10.2	8.7	8.3
NPV (k€)	14.7	11.5	10.7

C. *Tower layout #3 (TW3)*

Tower in the layout #3 (TW3) has a hexagonal section. Two commercial towers are considered, with 24 m and 30 m height, respectively. The installation of modules in two conditions is simulated: actually, PV generators can be inclined (with a metallic support linked to the tower) or vertically installed. Fig. 8 shows the 3D models of the two installations. The inclined modules have a tilt angle of 35° when south oriented, while the modules of the SE-SO sides have a tilt angle of 25°. The number of modules on the towers are shown in Table V. In addition, 18 modules are installed on the canopy.

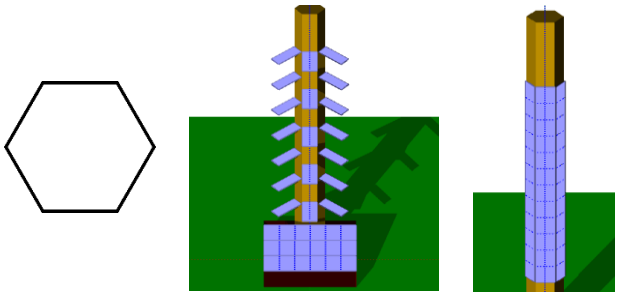

Fig. 8. Cross section of tower TW3 (left) and its 3D model with inclined PV modules (center) and vertical PV modules (right).

TABLE V. NUMBER OF MODULES INSTALLED ON THE TW3

Modules	Tower height 24 m	Tower height 30 m
Inclined	11	19
Vertical	21	36

The best results are obtained when the modules on the tower are inclined. The 24-meter height tower has a self-sufficiency in the range 23−27 %. The 30-meter height tower permits to install more modules; thus, self-sufficiency is higher (27−30 %). Regarding financial feasibility, all the solutions have a high *IRR* (in the range 9−12 %).

TABLE VI. RESULTS FOR TW3 IN THE THREE SITES (HEIGHT 24 M)

	Site#1	Site#2	Site#3
PV power (kW)	11	11	11
Production (MWh/year)	14.7	14.1	13.7
Self-sufficiency (%)	27	23	27
IRR (%)	12.2	11.6	10.6
NPV (k€)	20.0	18.6	16.3

TABLE VII. RESULTS FOR TW3 IN THE THREE SITES (HEIGHT 30 M)

	Site#1	Site#2	Site#3
PV power (kW)	13.7	13.7	13.7
Production (MWh/year)	18.1	17.5	17.0
Self-sufficiency (%)	30	27	30
IRR (%)	10.4	10.1	9.1
NPV (k€)	21.3	20.2	17.1

This highest tower is simulated also with the installation of batteries to store the surplus energy and use it during night hours. Their specifications are the following: the charging efficiency $\eta_{bat,c}$ is 90 %, the maximum number of cycles is 10 000, the *SOC* is supposed to be in the range 20 %–100 % [min–max], and the maximum power charging or discharging the batteries is 2 kW. An example of hourly energy flows is shown in Fig. 9: batteries are charged in the hours at sun peak and discharged in the evening. If they cannot satisfy all the night load, the deficit energy is absorbed by the grid. At midday, if generation is higher than load and batteries are full, the surplus is injected into the grid. In Site#1 and Site#3, the optimal size of the batteries is 16 kWh.

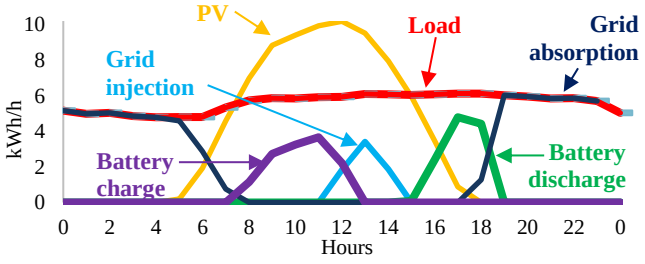

Fig. 9. Example of hourly energy flows with battery charge-discharge.

In Site#2, a high storage capacity is useless, because PV generation and surplus are low with respect to the load. For all these configurations, the storage increases *SS* up to 31–35 %, while the *IRR* decreases due to the high investment cost of batteries, and their replacement after 10 years.

TABLE VIII. RESULTS FOR TW3 IN THE THREE SITES (HEIGHT 30 M) WITH ELECTROCHEMICAL STORAGE

	Site#1	Site#2	Site#3
PV power (kW)	13.7	13.7	13.7
Storage size (kWh)	16	8	16
Production (MWh/year)	18.1	17.5	17.0
Self-sufficiency (%)	34	31	35
IRR (%)	7.2	8.4	6.0
NPV (k€)	13.7	16.4	9.7

V. CONCLUSIONS

The present work describes the sizing of PV-battery systems to increase self-sufficiency for telecommunication stations. The sizing procedure faces the problem of the low available space for PV modules and the high electric consumption. For these reasons, the study considered the installation of PV modules on the surfaces of the towers, and on a canopy protecting the electronic equipment. To increase as much as possible the production, it was supposed to replace the existing towers with new ones. Thus, more than ten different PV modules arrangements were investigated and different towers were approximated by 3D models to define the number of installable PV modules. The PV generators reached a rated power of 13.7 kW and permit to obtain a self-sufficiency of ≈30 % in their best configuration. The investment was effective with *IRR* ≈ 9–10 %. In order to furtherly increase the self-sufficiency, electrochemical storage was simulated to fulfil local loads first. The storage increased self-sufficiency up to 35 % in the best site; nevertheless, the *IRR* decreased down to 6 % due to the current cost of batteries.

REFERENCES

[1] F. Spertino, A. Ciocia, P. Di Leo, S. Fichera, G. Malgaroli and A. Ratclif, "Toward the Complete Self-Sufficiency of an nZEBs Microgrid by Photovoltaic Generators and Heat Pumps: Methods and Applications," in IEEE Transactions on Industry Applications, vol. 55, no. 6, pp. 7028-7040, 2019.

[2] A. Ciocia, P. Di Leo, S. Fichera, F. Giordano, G. Malgaroli and F. Spertino, "A Novel Procedure to Adjust the Equivalent Circuit Parameters of Photovoltaic Modules under Shading," 2020 International SPEEDAM, 2020, pp. 711-715.

[3] K. Lappalainen, S. Valkealahti, Effects of PV array layout, electrical configuration and geographic orientation on mismatch losses caused by moving clouds, Solar Energy, Volume 144, 2017, Pages 548-555.

[4] N. R. Deevela, B. Singh and T. C. Kandpal, "Load Profile of Telecom Towers and Potential Renewable Energy Power Supply Configurations," 2018 IEEE International PEDES, 2018, pp. 1-6.

[5] G. Modi and B. Singh, "Solar PV Battery Based System for Telecom Tower Application," 2020 IEEE ECCE, 2020, pp. 3065-3072.

[6] I. A. Ibrahim, S. Sabah, R. Abbas, M. J. Hossain, and H. Fahed, "A novel sizing method of a standalone photovoltaic system for powering a mobile network base station using a multi-objective wind driven optimization algorithm", Energy Convers. Manag., vol. 238, p. 114179, Jun. 2021.

[7] Ciocia, A.; Ahmad, J.; Chicco, G.; Di Leo, P.; Spertino, F. Optimal size of photovoltaic systems with storage for office and residential loads in the Italian net-billing scheme. In Proceedings of the 51st International UPEC, Coimbra, Portugal, 6–9 September 2016; pp. 1–6.

[8] Schujman S. B.; Mann J. R.; Dufresne G.; LaQue L. M.; Rice C.; Wax J.; Metacarpa D. J.; Haldar P. Evaluation of protocols for temperature coefficient determination. In Proceedings of the 2015 IEEE 42nd PVSC, New Orleans, LA, USA, 14–19 June 2015; pp. 1–4.

[9] Ould Amrouche, S.; Rekioua, D.; Rekioua, T.; Bacha, S. Overview of energy storage in renewable energy systems. *Int. J. Hydrog. Energ.* 2016, *41*, 20914–20927.

[10] Téllez Molina, M.B.; Prodanovic, M. Profitability assessment for self-sufficiency improvement in grid-connected non-residential buildings with on-site PV installations, in 2013 International ICCEP, Alghero, Italy, 11–13 June 2013; pp. 353–360.

[11] Italian Law, DM 04/07/2019. Accesso agli Incentivi. Available online: https://www.gse.it/servizi-per-te/fonti-rinnovabili/fer-elettriche/incentivi-dm-04-07-2019.

[12] Lin C.; Hsieh W.; Chen C.; Hsu C.; Ku T. Optimization of Photovoltaic Penetration in Distribution Systems Considering Annual Duration Curve of Solar Irradiation. *IEEE Trans. Power Syst*. **2012**, *27*, 1090–1097.

[13] Photovoltaic Geographical Information System (PVGIS). Available online: https://ec.europa.eu/jrc/en/pvgis (accessed on 19 Jan 2022).

[14] Issi F, Kaplan O. The Determination of Load Profiles and Power Consumptions of Home Appliances. Energies. 2018; 11(3):607.

[15] Liu S.; Dong M. Quantitative research on impact of ambient temperature and module temperature on short-term photovoltaic power forecasting, Intern. Conf. on Smart Grid and Clean Energy Technologies, Chengdu, China, 19–22 Oct 2016; pp. 262–266.

[16] F. Spertino, A. Ciocia, P. Di Leo, R. Tommasini e I. Berardone, M. Corrado, A. Infuso, M. Paggi, «A power and energy procedure in operating photovoltaic systems to quantify the losses according to the causes» Solar Energy, vol. 118, 2015.

[17] National Renewable Energy Laboratory of U.S.A. Photovoltaic Degradation Rates, An Analytical Review. Online: https://www.nrel.gov/docs/fy12osti/51664.pdf.

[18] Carullo, A.; Castellana, A.; Vallan, A.; Ciocia, A.; Spertino, F. In-field monitoring of eight photovoltaic plants: Degradation rate over seven years of continuous operation. *Acta IMEKO* 2018, *7*, 75–81.

[19] International Energy Agency, "Renewables 2020, Solar PV", Online: https://www.iea.org/reports/renewables-2020/solar-pv

[20] European Commission. Regulation 2017/2195 of 23 Nov 2017 Establishing a Guideline on Electricity Balancing. Available online: http://data.europa.eu/eli/reg/2017/2195/oj.

[21] U.S. Energy Information Administration, "Levelized Cost and Levelized Avoided Cost of New Generation Resources in the Annual Energy Outlook 2016," Available online: http://www.eia.gov/outlooks/aeo/pdf/electricity_generation.pdf.

[22] GSE. Servizio di Scambio sul posto: Regole Tecniche. Avail. online: www.gse.it/documenti_site/Documenti%20GSE/Servizi%20per%20te/SCAMBIO%20SUL%20POSTO/Regole%20e%20procedure/Regole%20Tecniche%20Scambio%20sul%20Posto_2019.pdf.

[23] Spertino F, Amato A, Casali G, Ciocia A, Malgaroli G. Reliability Analysis and Repair Activity for the Components of 350 kW Inverters in a Large Scale Grid-Connected Photovoltaic System. *Electronics*. 2021; 10(5):564.

[24] A.F. Murtaza, H.A. Sher, M. Chiaberge, D. Boero, M. De Giuseppe, K.E. Addoweesh, A novel hybrid MPPT technique for solar PV applications using perturb & observe and fractional open circuit voltage techniques. 15th International Conference Mechatronika, Prague, Czech Republic, 5–7 December 2012; pp. 1–8.

[25] F. Spertino, J. Ahmad, A. Ciocia and P. Di Leo, "A technique for tracking the global maximum power point of photovoltaic arrays under partial shading conditions," 2015 IEEE 6th PEDG, 2015, pp. 1-5.

[26] A. F. Murtaza, H. A. Sher, K. Al-Haddad and F. Spertino, "Module Level Electronic Circuit Based PV Array for Identification and Reconfiguration of Bypass Modules," in IEEE Transactions on Energy Conversion, vol. 36, no. 1, pp. 380-389, March 2021.

[27] Ciocia A, Amato A, Di Leo P, Fichera S, Malgaroli G, Spertino F, Tzanova S. Self-Consumption and Self-Sufficiency in Photovoltaic Systems: Effect of Grid Limitation and Storage Installation. *Energies*. 2021; 14(6):1591.

[28] Mazza A, Mirtaheri H, Chicco G, Russo A, Fantino M. Location and Sizing of Battery Energy Storage Units in Low Voltage Distribution Networks. *Energies*. 2020; 13(1):52.